HOKKAIDO UNIVERSITY

Title	Chaotic motion of the N-vortex problem on a sphere: II. Saddle centers in three-degree-of-freedom Hamiltonians
Author(s)	Sakajo, Takashi; Yagasaki, Kazuyuki
Citation	Physica D Nonlinear Phenomena, 237(14-17), 2078-2083 https://doi.org/10.1016/j.physd.2008.02.001
Issue Date	2008-08-15
Doc URL	http://hdl.handle.net/2115/34774
Type	article (author version)
File Information	EE250_PhysDh.pdf

Instructions for use

Hokkaido University Collection of Scholarly and Academic Papers : HUSCAP

Chaotic motion of the N-vortex problem on a sphere: II. Saddle centers in three-degree-of-freedom Hamiltonians

Takashi Sakajo[1,*] and Kazuyuki Yagasaki[2]

[1] Department of Mathematics, Hokkaido University, Sapporo 060-0810, JAPAN

[2] Department of Mechanical and Systems Engineering, Gifu University, Gifu 501-1193, JAPAN

This paper deals with complicated behavior in the $N = 8n$ vortex problem on a sphere, which is reduced to three-degree-of-freedom Hamiltonian systems. In the reduced Hamiltonians, the polygonal ring configuration of the point vortices becomes a saddle-center equilibrium which has two hyperbolic and four center directions in some parameter regions. Near the saddle-center, there exists a normally hyperbolic, locally invariant manifold including a Cantor set of *whiskered tori*. For $N = 8$ we numerically compute the stable and unstable manifolds of the locally invariant manifold with assistance of the center manifold technique, and show that they intersect transversely and complicated dynamics may occur. Direct numerical simulations are also given to demonstrate our numerical analysis.

PACS numbers: 47.10.A-,47.15.ki

I. INTRODUCTION

We consider the motion of N point vortices with the unit strength on a sphere. Their equations of motion are derived from the two-dimensional incompressible Euler equations on the sphere by assuming that the vorticity is concentrated at discrete points (Θ_m, Ψ_m), $m = 1, \ldots, N$, in the spherical coordinates. They can be written in a Hamiltonian system with N degrees of freedom [14]:

$$\dot{q}_m = \frac{\partial H}{\partial p_m}, \quad \dot{p}_m = -\frac{\partial H}{\partial q_m}, \tag{1}$$

where $(q_m, p_m) = (\Psi_m, \cos\Theta_m)$ are the symplectic variables. The Hamiltonian H is given by

$$H = -\frac{\Gamma_{\rm n}}{4\pi}\sum_{m=1}^{N}\log(1-\cos\Theta_m) - \frac{\Gamma_{\rm s}}{4\pi}\sum_{m=1}^{N}\log(1+\cos\Theta_m)$$
$$-\frac{1}{4\pi}\sum_{m=1}^{N}\sum_{m<j}^{N}\log(1-\cos\gamma_{mj}), \tag{2}$$

in which γ_{mj} denotes the central angle between the mth and jth point vortices such that $\cos\gamma_{mj} = \cos\Theta_m\cos\Theta_j - \sin\Theta_m\sin\Theta_j\cos(\Psi_m - \Psi_j)$. The parameters $\Gamma_{\rm n}$ and $\Gamma_{\rm s}$ represent the strengths of the point vortices fixed at the north and the south poles of the sphere, which are introduced to incorporate with an effect of rotation of the sphere locally. The *N-vortex problem* on the sphere including (1) has been extensively studied when N is small. For instance, the integrable 3-vortex problem and an integrable 4-vortex problem were discussed in detail [10, 18, 22]. See [14] for further references on this topic.

Now, we focus on the evolution of the polygonal ring configuration, called the *N-ring*, where the point vortices are equally spaced along a line of latitude when N is not small. The configuration is of significance since such coherent vortex structure is often observed in numerical simulations on planetary flows [16, 19]. The N-ring, $\Theta_m = \theta_0$ and $\Psi_m = 2\pi m/N$, is a relative equilibrium of (1) rotating with a constant speed in the longitudinal direction. Such relative fixed configurations with special symmetries were investigated in a systematic way [11] and its stability has been investigated very well [2, 3, 20]. Here we are interested in how the N-ring evolves when it becomes unstable. In general, it is difficult to describe the evolution of many point vortices since the degree of freedom of the system is quite large. However, the Hamiltonian system (1) can often be reduced to a lower dimensional system in a systematic way [21].

For $N = 5n, 6n$ with $n \in \mathbb{N}$, using the reduction method, we obtain a two-degree-of-freedom Hamiltonian system that has a saddle-center equilibrium with two hyperbolic and two center directions for some regions of $\Gamma_{\rm n} = \Gamma_{\rm s}$. Near the saddle-center there is a one-parameter family of periodic orbits by the Lyapunov center theorem [12], and their stable and unstable manifolds may intersect transversely so that horseshoe-type chaotic dynamics occurs. We applied a global perturbation technique [26] for $N = 6$ and used a numerical technique [29] for $N = 5, 6$ to detect such transverse intersections [23]. These treatments can also be performed for the general cases of $N = 5n, 6n$.

In the present paper, as a sequel to the previous work [23], we study complicated dynamics of the $N = 8n$ vortex problem when the N-ring is a saddle-center. We first reduce (1) to a three-degree-of-freedom Hamiltonian system. Near the saddle-center, instead of a one-parameter family of periodic orbits, there is a normally hyperbolic, locally invariant manifold including a Cantor set of *whiskered tori*, and its stable and unstable manifolds may also intersect, so that complicated dynamics can occur [28] (see also Sec. II). An analytical technique similar to that of [26] was also developed to treat this

*Electronic address: sakajo@math.sci.hokudai.ac.jp

situation in [28] but is not applicable in our case. So we use the numerical technique of [29] with assistance of the center manifold technique [7] to show numerically that such intersection really occurs.

This paper is organized as follows: In Sec. II, we apply the reduction method of [21] to (1) for $N = 8n$ and discuss complicated dynamics resulting from intersection between the stable and unstable manifolds of the locally invariant manifold. In Sec. III, we introduce some symplectic transformations to make the problem amenable to our analysis. In Sec. IV we describe the center manifold calculation and numerical technique to compute the stable and unstable manifolds of the locally invariant manifold. In Sec. V we perform the numerical analysis for $N = 8$ and give direct numerical simulations that support our analytical results relying on numerics. We conclude with a summary and comments in Sec. VI.

II. INVARIANT DYNAMICAL SYSTEMS IN THE $N = 8n$ VORTEX PROBLEM

Linear stability analysis of the N-ring [20] gives the explicit representation of the eigenvalues. Let $\lambda_m^\pm$, $m = 0, \ldots, N$, denote the eigenvalues for the N-ring equilibrium. Suppose that N is even and set $N = 2M$. Since $\lambda_0^\pm = 0$ and $\lambda_m^\pm = \lambda_{N-m}^\pm$, we see that $\lambda_M^\pm$ are simple and $\lambda_m^\pm$ are double for $m = 1, \cdots, M-1$. Since $\left(\lambda_i^\pm\right)^2 < \left(\lambda_j^\pm\right)^2$ for $1 \le i < j \le M$, we have $\left(\lambda_k^\pm\right)^2 < 0 < \left(\lambda_{k+1}^\pm\right)^2$ for some k so that $\lambda_m^\pm$ are neutrally stable for $m \le k$ and λ_m^+ (resp. λ_m^-) is unstable (resp. stable) for $m > k$.

We define two transformations for the configuration $(\Theta_1, \ldots, \Theta_N, \Psi_1, \ldots, \Psi_N) \in \mathbb{P}_N = [0,\pi]^N \times (\mathbb{R}/2\pi\mathbb{Z})^N$. The first transformation rotates the point vortices by the degree $2\pi p/N$, which is denoted by $\sigma_p : (\Theta_1, \ldots, \Theta_N, \Psi_1, \ldots, \Psi_N) \mapsto (\Theta_1', \ldots, \Theta_N', \Psi_1', \ldots, \Psi_N')$, where $\Theta_m' = \Theta_{N-p+m}$, $\Psi_m' = \Psi_{N-p+m} + 2\pi p/N$ for $m = 1, \cdots, p$ and $\Theta_m' = \Theta_{m-p}$, $\Psi_m' = \Psi_{m-p} + 2\pi p/N$ for $m = p+1, \cdots, N$. The second one is the pole reversal transformation that reverses the north and the south poles around the x-axis; For $N = 2M$, it is given by $\pi_\mathrm{e} : (\Theta_1, \ldots, \Theta_N, \Psi_1, \ldots, \Psi_N) \mapsto (\Theta_1'', \ldots, \Theta_N'', \Psi_1'', \ldots, \Psi_N'')$, where $\Theta_1'' = \pi - \Theta_1$, $\Psi_1'' = \Psi_1$, $\Theta_m'' = \pi - \Theta_{N-m+2}$ and $\Psi_m'' = 2\pi + 2\Psi_1 - \Psi_{N-m+2}$ for $m \neq 1$.

Let $\boldsymbol{\phi}_m^\pm$, $m = 1, \cdots, M-1$, be the linear independent eigenvectors to $\lambda_m^\pm$, which were also given explicitly in [20]. Then we have the following result [21].

Proposition 1. *Let $N = 2M = pq$ ($p, q \in \mathbb{N}$) and let $\Gamma_\mathrm{n} = \Gamma_\mathrm{s}$. If $\sigma_p \pi_\mathrm{e} \boldsymbol{X}(0) = \boldsymbol{X}(0)$ for $\boldsymbol{X} \in \mathbb{P}_N$, then $\sigma_p \pi_\mathrm{e} \boldsymbol{X}(t) = \boldsymbol{X}(t)$ for $t \ge 0$. Furthermore, the set of*

$$\boldsymbol{X} = \boldsymbol{X}_\mathrm{e} + \sum_k \left(b_k^+ \boldsymbol{\phi}_{kq}^+ + b_k^- \boldsymbol{\phi}_{kq}^- \right), \quad b_k^\pm \in \mathbb{R}, \tag{3}$$

is invariant with respect to $\sigma_p \pi_\mathrm{e}$, where $\boldsymbol{X}_\mathrm{e}$ represents the N-ring at the equator.

Note that the dimension of the vector space (3) is $[(M-1)/q]$ since the number of eigenvectors $\boldsymbol{\phi}_m^\pm$ is $M-1$, where $[r]$ denotes the maximum integer that is less than or equals to r. Henceforth we set $\Gamma_\mathrm{n} = \Gamma_\mathrm{s} = \Gamma$.

Applying Proposition 1 to the case of $N = 8n$, i.e. $p = 8$, $q = n$ and $M = 4n$, we obtain a reduced Hamiltonian system with three degrees of freedom in which $\lambda_n^\pm$, $\lambda_{2n}^\pm$ and $\lambda_{3n}^\pm$ are eigenvalues for an equilibrium corresponding the N ring. Moreover, for a certain region of Γ, we have $\left(\lambda_n^\pm\right)^2 < \left(\lambda_{2n}^\pm\right)^2 < 0 < \left(\lambda_{3n}^\pm\right)^2$ so that the equilibrium becomes a saddle-center since $\lambda_{3n}^\pm$ are real with $\lambda_{3n}^- < 0 < \lambda_{3n}^+$ while $\lambda_n^\pm$ and $\lambda_{2n}^\pm$ are purely imaginary.

In this situation, we can apply a slight modification of discussions given in [28]. The saddle-center has a four-dimensional center manifold, which we regard as a normally hyperbolic, locally invariant manifold $\mathscr{M}$ having five-dimensional stable and unstable manifolds $W^{\mathrm{s,u}}(\mathscr{M})$. Here “normal hyperbolicity” means that the expansion and contraction rates of the flow normal to $\mathscr{M}$ dominate those tangent to $\mathscr{M}$, and “local invariance” means that some trajectories starting in $\mathscr{M}$ may escape $\mathscr{M}$ through its boundary $\partial\mathscr{M}$. See, e.g., [25] for the details of these concepts. Using the normal form of Graff [6] and applying the KAM theorem [13] (see also [17]), we can show that there exists a Cantor set of invariant tori near the saddle-center. Each invariant torus $\mathscr{T}$ is *whiskered* and has three-dimensional stable and unstable manifolds $W^\mathrm{s}(\mathscr{T})$ and $W^\mathrm{u}(\mathscr{T})$, which are contained by $W^\mathrm{s}(\mathscr{M})$ and $W^\mathrm{u}(\mathscr{M})$, respectively.

Suppose that $W^\mathrm{s}(\mathscr{M})$ and $W^\mathrm{u}(\mathscr{M})$ intersect transversely. Then for any $K > 2$, there may be a *transition chain* of K whiskered tori, $\mathscr{T}_j$, $j = 1, \ldots, K$, on $\mathscr{M}$ near the saddle-center, such that $W^\mathrm{u}(\mathscr{T}_j)$ intersects $W^\mathrm{s}(\mathscr{T}_{j+1})$ for $j = 1, \ldots, K-1$. It follows that there exist trajectories starting near $\mathscr{T}_1$, passing near $\mathscr{T}_j$, $j = 2, \ldots, K-1$, in turn and arriving near $\mathscr{T}_K$: “diffusion motions” occur. Moreover, there may be a pair of distinct *heteroclinic cycles*, $\{\mathscr{T}_0, \mathscr{T}_1^j, \ldots, \mathscr{T}_{K_j}^j, \mathscr{T}_0\}$ with $K_j \ge 1$, $j = 1, 2$ among the transition chains. So we can find trajectories which start in a neighborhood of $\mathscr{T}_0$ and return there repeatedly after they pass near $\mathscr{T}_1^1, \ldots, \mathscr{T}_{K_1}^1$ or near $\mathscr{T}_1^2, \ldots, \mathscr{T}_{K_2}^2$. These trajectories can be assigned the symbols ‘1’ or ‘2’ depending whether they pass near $\mathscr{T}_1^1, \ldots, \mathscr{T}_{K_1}^1$ or near $\mathscr{T}_1^2, \ldots, \mathscr{T}_{K_2}^2$. Thus, they can be characterized by the Bernoulli shift and hence chaotic dynamics occurs. This also implies that chaotic drift of trajectories occurs in the center directions of the saddle-center. See [28] for more details.

Thus, the transverse intersection between $W^\mathrm{s}(\mathscr{M})$ and $W^\mathrm{u}(\mathscr{M})$ indicates complicated dynamics. We especially note that the complicated motions are not confined to a small neighborhood of the saddle-center but rather global ones. In the following, we focus on a special case of $N = 8$ and numerically show the occurrence of such intersection in the reduced system since the analytical technique of [28] is not applicable. Before that, as in [23], we modify the reduced system by symplectic transformations so that it becomes amenable to our analysis, in the next section.

III. SYMPLECTIC TRANSFORMATIONS FOR $N = 8$

Since σ_8 is the identity map for $N = 8$ so that $\sigma_8\pi_{\rm e} = \pi_{\rm e}$, we reduce the system (1) via Proposition 1 to a $\pi_{\rm e}$-invariant three-degree-of-freedom Hamiltonian system whose phase space (3) is represented by

$$\boldsymbol{X} = \boldsymbol{X}_{\rm e} + \sum_{k=1}^{3}(b_k^+\boldsymbol{\phi}_k^+ + b_k^-\boldsymbol{\phi}_k^-), \quad b_{1,2,3}^{\pm} \in \mathbb{R}. \tag{4}$$

As in [23], introducing the generating function

$$W(P_m, q_m) = P_1 q_1 + \sum_{m=2}^{8} P_m(q_m - q_{m-1}), \tag{5}$$

we define a symplectic transformation $(q_m, p_m) \mapsto (Q_m, P_m)$. It follows directly from the definition of $\pi_{\rm e}$ that $\pi_{\rm e}$-invariant orbits satisfy

$$\begin{aligned} &q_1 = 0, \quad q_5 = \pi, \quad q_m + q_{10-m} = 2\pi,\\ &p_1 = p_5 = 0, \quad p_m + p_{10-m} = 0 \end{aligned} \tag{6}$$

for $m = 2, 3, 4$. Since in the symplectic transformation generated by (5)

$$\begin{aligned} &q_2 = 2\pi - Q_3 - Q_4 - Q_5, \quad q_3 = 2\pi - Q_4 - Q_5,\\ &q_4 = 2\pi - Q_5, \quad p_2 = -P_3, \quad p_3 = P_3 - P_4,\\ &p_4 = P_4 - P_5, \end{aligned} \tag{7}$$

the reduced Hamiltonian system is represented by (Q_m, P_m) with $m = 3, 4, 5$ and the 8-ring becomes $Q_m = \pi/4$ and $P_m = 0$.

We further introduce the symplectic transformation

$$\begin{aligned} Q_3 =& \tfrac{1}{4}(\pi + (1+\sqrt{2})x_1 + 2y_1 + (1-\sqrt{2})y_2),\\ Q_4 =& \tfrac{1}{4}(\pi - (1+\sqrt{2})x_1 + 2y_1 - (1-\sqrt{2})y_2),\\ Q_5 =& \tfrac{1}{4}(\pi + x_1 - 2y_1 + y_2),\\ P_3 =& x_2 + y_3 + y_4,\\ P_4 =& (1-\sqrt{2})x_2 + y_3 + (1+\sqrt{2})y_4,\\ P_5 =& (2-\sqrt{2})x_2 + (2+\sqrt{2})y_4, \end{aligned} \tag{8}$$

so that the 8-ring becomes the origin O and the eigenspaces for the saddle and center eigenvalues correspond to the $\boldsymbol{x}$-plane and $\boldsymbol{y}$-hyperplane, respectively. Thus, we finally obtain the Hamiltonian system

$$\dot{\boldsymbol{x}} = J_1 \mathrm{D}_x H(\boldsymbol{x}, \boldsymbol{y}), \quad \dot{\boldsymbol{y}} = J_2 \mathrm{D}_y H(\boldsymbol{x}, \boldsymbol{y}), \tag{9}$$

where J_m is the $2m \times 2m$ symplectic matrix,

$$J_m = \begin{pmatrix} 0 & \mathrm{id}_m \\ -\mathrm{id}_m & 0 \end{pmatrix}$$

with id_m the $m \times m$ identity matrix. The expression of $H(\boldsymbol{x}, \boldsymbol{y})$ is easily obtained by substituting (7) and (8) into (2) under the constraints (6), but it is too lengthy to present in the paper.

Let us assume that $5/2 \le \Gamma \le 4$. Then the 8-ring corresponds to a saddle-center equilibrium in (9) since $(\lambda_1^{\pm})^2 < (\lambda_2^{\pm})^2 < 0 < (\lambda_3^{\pm})^2$. Moreover, there exists an unstable direction associated with $\lambda_4^+ > 0$ and normal to the invariant space (4). However, we expect that some solutions of the full system (1) exhibit similar motions for a period repeatedly when chaotic motions occur in the reduced system (9), since by the Poincaré recurrence theorem [1], they must repeatedly return in a neighborhood of the invariant space if they start there.

IV. NUMERICAL COMPUTATION OF $W^{\rm s,u}(\mathscr{M})$

Now we describe our approach for numerical computation of $W^{\rm s,u}(\mathscr{M})$ in (9) when $\mathscr{M}$ is in a small neighborhood of O. Other methods for such computation are also available [9, 24], but ours is simpler and easier to perform and provides precise results, as we see below.

We begin with a standard asymptotic expansion method [7] to compute the center manifold of the saddle-center at the origin approximately up to $\mathscr{O}(|\boldsymbol{y}|^3)$ as

$$\mathscr{M} = \{(\boldsymbol{x}, \boldsymbol{y}) \in \mathbb{R}^2 \times \mathbb{R}^4 \mid \boldsymbol{x} = \boldsymbol{h}(\boldsymbol{y})\}, \tag{10}$$

where $\boldsymbol{h}(\boldsymbol{y}) = (h_1(\boldsymbol{y}), h_2(\boldsymbol{y}))^{\rm T}$ with

$$\begin{aligned} h_1(\boldsymbol{y}) =& b_{1100}^{(1)} y_1 y_2 + b_{0011}^{(1)} y_3 y_4 + b_{0300}^{(1)} y_2^3 + b_{2100}^{(1)} y_1^2 y_2\\ &+ b_{0120}^{(1)} y_2 y_3^2 + b_{0102}^{(1)} y_2 y_4^2 + b_{1011}^{(1)} y_1 y_3 y_4,\\ h_2(\boldsymbol{y}) =& b_{1001}^{(2)} y_1 y_4 + b_{0110}^{(2)} y_2 y_3 + b_{0003}^{(2)} y_4^3 + b_{2001}^{(2)} y_1^2 y_4\\ &+ b_{0201}^{(2)} y_2^2 y_4 + b_{0021}^{(2)} y_3^2 y_4 + b_{1110}^{(2)} y_1 y_2 y_3 \end{aligned} \tag{11}$$

(see Appendix A for the coefficients in (11)). Thus, we can approximate (9) near the origin as

$$\dot{\boldsymbol{\xi}} = \boldsymbol{J}_1 \mathrm{D}_x^2 H_4(\boldsymbol{h}(\boldsymbol{y}), \boldsymbol{y})\boldsymbol{\xi}, \quad \dot{\boldsymbol{y}} = \boldsymbol{J}_2 \mathrm{D}_y H_4(\boldsymbol{h}(\boldsymbol{y}), \boldsymbol{y}), \tag{12}$$

where $H_4(\boldsymbol{x}, \boldsymbol{y})$ is the fourth-order polynomial approximation of the Hamiltonian $H(\boldsymbol{x}, \boldsymbol{y})$ and $\boldsymbol{\xi} = \boldsymbol{x} - \boldsymbol{h}(\boldsymbol{y})$.

Using the numerical technique of [29] with assistance of the approximation (12), we compute the unstable manifold $W^{\rm u}(\mathscr{M})$ as follows. We first numerically solve (12) on a time-interval $[-T, 0]$ to obtain a small trajectory $\bar{\boldsymbol{y}}(t)$ on $\mathscr{M}$ near the origin O and its one-dimensional unstable subspace $E^{\rm u} \subset \mathbb{R}^2$ for $\bar{\boldsymbol{y}}(t)$ at $t = 0$ such that $\boldsymbol{\xi}(t) \to \boldsymbol{0}$ as $t \to -\infty$ if $\boldsymbol{\xi}(0) \in E^{\rm u}$. Let $\boldsymbol{e}^{\rm u}$ be a unit vector spanning $E^{\rm u}$, which is approximated as

$$\boldsymbol{e}^{\rm u} \approx \boldsymbol{\xi}(0)/|\boldsymbol{\xi}(0)|, \quad \boldsymbol{\xi}(\bar{T}) = \boldsymbol{\xi}_0 \tag{13}$$

if $\bar{T}$ is large and $(\boldsymbol{\xi}_0, \boldsymbol{0})$ is the unstable eigenvector of O in (9), as shown in [29]. We compute a trajectory $(\boldsymbol{x}^{\rm u}(t), \boldsymbol{y}^{\rm u}(t))$ on $W^{\rm u}(\mathscr{M})$ by solving (9) under the boundary conditions

$$\begin{aligned} &\boldsymbol{x}^{\rm u}(0) - \boldsymbol{h}(\boldsymbol{y}^{\rm u}(0)) = \varepsilon_{\rm u}\boldsymbol{e}^{\rm u}, \quad \boldsymbol{y}^{\rm u}(0) = \bar{\boldsymbol{y}}(0),\\ &(\boldsymbol{x}^{\rm u}(T_{\rm u}), \boldsymbol{y}^{\rm u}(T_{\rm u})) = (\boldsymbol{x}_0^{\rm u}, \boldsymbol{y}_0^{\rm u}), \end{aligned} \tag{14}$$

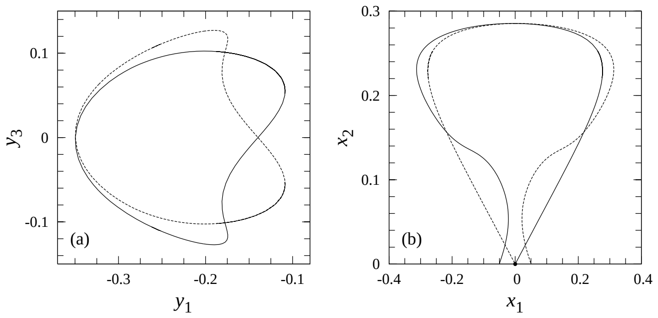

FIG. 1: Intersection of the unstable and stable manifolds $W^{\mathrm{s,u}}(\mathscr{M})$ with the section $\{x_1 = y_2 = y_4 = 0\}$ or $\{y_2 = y_3 = y_4 = 0\}$ for $\Gamma = 3$ on the energy level $\Delta H = 5 \times 10^{-3}$: (a) Their projections onto the (y_1, y_3)-plane; (b) onto the $\boldsymbol{x}$-plane. The solid and broken lines represent the stable and unstable manifolds, respectively. In plate (b), '•' represents the saddle-center at the origin.

where $\varepsilon_{\mathrm{u}} \ll 1$ and T_{u} are positive constants, and $(\boldsymbol{x}_0^{\mathrm{u}}, \boldsymbol{y}_0^{\mathrm{u}}) \in \mathbb{R}^2 \times \mathbb{R}^4$ represents an approximate point on $W^{\mathrm{u}}(\mathscr{M})$. Thus, numerical continuation of the solutions $(\boldsymbol{\xi}(t), \bar{\boldsymbol{y}}(t))$ and $(\boldsymbol{x}^{\mathrm{u}}(t), \boldsymbol{y}^{\mathrm{u}}(t))$ for the boundary value problem (9), (12) and (14) gives $W^{\mathrm{u}}(\mathscr{M})$. Similarly, we compute $W^{\mathrm{s}}(\mathscr{M})$ by continuing a solution $(\boldsymbol{\xi}(t), \bar{\boldsymbol{y}}(t))$ of (12) on $[0, \bar{T}]$ and a solution $(\boldsymbol{x}^{\mathrm{s}}(t), \boldsymbol{y}^{\mathrm{s}}(t))$ of (9) satisfying the boundary conditions

$$\begin{aligned} &\boldsymbol{x}^{\mathrm{s}}(0) - \boldsymbol{h}(\boldsymbol{y}^{\mathrm{s}}(0)) = \varepsilon_{\mathrm{s}} \boldsymbol{e}^{\mathrm{s}}, \quad \boldsymbol{y}^{\mathrm{s}}(0) = \bar{\boldsymbol{y}}(0), \\ &(\boldsymbol{x}^{\mathrm{s}}(-T_{\mathrm{s}}), \boldsymbol{y}^{\mathrm{s}}(-T_{\mathrm{s}})) = (\boldsymbol{x}_0^{\mathrm{s}}, \boldsymbol{y}_0^{\mathrm{s}}), \end{aligned} \tag{15}$$

where $\boldsymbol{e}^{\mathrm{s}} \in \mathbb{R}^2$ is a unit vector spanning the one-dimensional stable subspace $E^{\mathrm{s}} \subset \mathbb{R}^2$ for $\bar{\boldsymbol{y}}(t)$ at $t = 0$ such that $\boldsymbol{\xi}(t) \to \boldsymbol{0}$ as $t \to \infty$ if $\boldsymbol{\xi}(0) \in E^{\mathrm{s}}$, where $\varepsilon_s \ll 1$ and T_{s} are positive constants, and $(\boldsymbol{x}_0^{\mathrm{s}}, \boldsymbol{y}_0^{\mathrm{s}}) \in \mathbb{R}^2 \times \mathbb{R}^4$ represents an approximate point on $W^{\mathrm{s}}(\mathscr{M})$. Note that as in (13), $\boldsymbol{e}^{\mathrm{s}}$ is approximated as

$$\boldsymbol{e}^{\mathrm{s}} \approx \boldsymbol{\xi}(0)/|\boldsymbol{\xi}(0)|, \quad \boldsymbol{\xi}(-\bar{T}) = \boldsymbol{\xi}_0 \tag{16}$$

if $\bar{T}$ is large and $(\boldsymbol{\xi}_0, \boldsymbol{0})$ is the stable eigenvector of O in (9).

To carry out the above computations of continuation, we use the computer tool "AUTO97" [5]. As the starting ones for the continuation, we take solutions of the linearized system for (12) at the origin (with $\bar{T}$ and $T_{\mathrm{s,u}}$ small), as in [23]. In the continuation $\bar{T}$, $T_{\mathrm{s,u}}$, $\boldsymbol{x}_0^{\mathrm{s,u}}$, $\boldsymbol{y}_0^{\mathrm{s,u}}$ or $\bar{\boldsymbol{y}}(\pm\bar{T})$ are chosen as the free parameters.

V. NUMERICAL RESULTS

Using the method of Sec. IV, we compute the stable and unstable manifolds $W^{\mathrm{s,u}}(\mathscr{M})$ in the reduced three-degree-of-freedom Hamiltonian system (9) for $N = 8$. Figure 1 shows an example of the numerical results for $\Gamma = 3$ and $\Delta H = H - H(\boldsymbol{0}, \boldsymbol{0}) = 5 \times 10^{-3}$. We see that these manifolds intersect transversely so that complicated dynamics may occur in (9), as described in Sec. II.

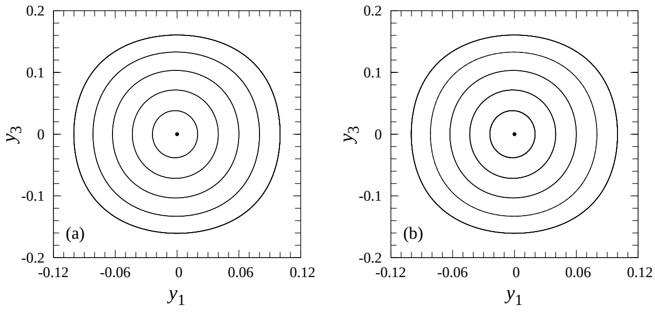

FIG. 2: Approximately computed orbits of the Poincaré map on the locally invariant manifold $\mathscr{M}$. The fourth-order approximate and exact Hamiltonian are used in plates (a) and (b), respectively.

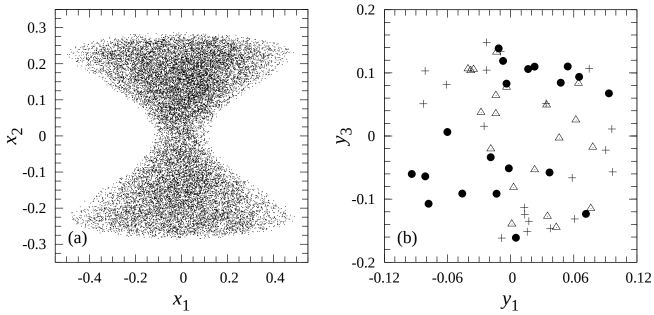

FIG. 3: Orbit of the Poincaré map: (a) Its projections onto the $\boldsymbol{x}$-plane; (b) onto the (y_1, y_3)-plane when it enters in a neighborhood of $\mathscr{M}$. In plate (b), '+' represents for 1st-20th visits, '•' for 21st-40th, and '△' for 41st-60th.

To demonstrate the occurrence of such complicated dynamics, we carry out direct numerical simulations using an approach similar to that of [23] and a computer software named "Dynamics" [15] with an adoption of a code named "DOP853" [8]. The code is based on the explicit Runge-Kutta method of order 8 by Dormand and Prince [4], a fifth order error estimator with third order correction is utilized and a dense output of order 7 is included. A small tolerance of 10^{-8} is chosen in the computations so that the numerical results are very accurate although the method is not symplectic. Below we set $\Gamma = 3$ and $\Delta H = 5 \times 10^{-3}$ as in Fig. 1, and often use the Poincaré map for the section $\{y_4 = 0, \dot{y}_4 > 0\}$.

Figure 2 shows approximately computed orbits of the Poincaré map on $\mathscr{M}$. Here the fourth-order approximate and exact Hamiltonian are used in Figs. 2(a) and (b), respectively, while the third-order approximation is used for $\mathscr{M}$ in both figures. We see that both results are almost the same and that all the computed orbits construct invariant tori. This also implies that our approximations made for computation of $W^{\mathrm{s,u}}(\mathscr{M})$ are appropriate.

Figure 3 shows a numerically computed orbit of the Poincaré map starting at $(\boldsymbol{x}, \boldsymbol{y}) =$

$(0.001, 0, 0.0861491, 0, 0.1, 0)$. Its projection onto the $\boldsymbol{x}$-plane is plotted with 20 000 points in Fig. 3(a), and its projection onto the (y_1, y_3)-plane when it enters in a neighborhood of $\mathscr{M}$, $\{|\boldsymbol{x} - \boldsymbol{h}(\boldsymbol{y})| < 0.01\}$, is plotted with 60 points in Fig. 3(b), where different symbols are used for every 20 visits. Note that the points of Fig. 3(a) are confined to some region since the energy level set is bounded. We observe that the orbit does not only exhibit a chaotic motion but also randomly drifts in the center directions of the saddle-center, as described in Sec. II. A numerical observation of such behavior in a three-degree-of-freedom Hamiltonian system was reported in [27] earlier.

Figure 4 shows a chaotic motion of the eight point vortices on the sphere, which is obtained by a solution of the reduced system (9) and corresponds to the orbits in Fig. 3. For comparison, we show a chaotic motion of the full system (1) without the π_e-symmetry in Fig. 5. Although the invariant space (4) is unstable, we see that the chaotic trajectory in the full system evolves like that in the reduced system, as predicted by the Poincaré recurrence theorem [1] (See Sec. III and also Sec. 7 of [23]).

VI. CONCLUSIONS

In this paper we have revealed that complicated dynamics exists in the $N = 8n$ vortex problem on a sphere. Our numerical analysis with assistance of the center manifold technique showed that the stable and unstable manifolds of a locally invariant manifold including a Cantor set of whiskered tori near the saddle-center N-ring equilibrium intersect transversely in the reduced Hamiltonian system. We gave numerical simulation results to demonstrate that complicated behavior resulting from such intersection occur in the Euler flow as well as in the reduced system. Thus, our dynamical systems approach sheds light on the new interesting feature of the important fluid problem, as in [23]. Finally, we remark that our treatment is also valid for $N = 7n$ as well as $N = 8n$ although the necessary center manifold calculations are tedious, and that the numerical technique is applicable to a large class of Hamiltonian systems with saddle-centers.

APPENDIX A: COEFFICIENTS OF (11)

Let

$$\begin{aligned}
\beta_1 =& 16\Gamma^2 - 54\Gamma - 45,\\
\beta_2 =& 128\Gamma^4 - 1232\Gamma^3 + 1140\Gamma^2 + 6300\Gamma + 3375,\\
\beta_3 =& 256\Gamma^4 - 2304\Gamma^3 + 7740\Gamma^2 - 8100\Gamma - 10125,\\
\beta_4 =& 8(2\Gamma - 15)\beta_3.
\end{aligned}$$

The second-order coefficients are given by

$$\begin{aligned}
b^{(1)}_{1100} &= -\frac{4\Gamma^2 + 60\Gamma - 279}{4\beta_1},\\
b^{(1)}_{0011} &= -\frac{2(4\Gamma^3 - 60\Gamma^2 + 171\Gamma + 45)}{\beta_1},\\
b^{(2)}_{1001} &= \frac{5(4\Gamma^2 - 36\Gamma + 9)}{4\beta_1},\ b^{(2)}_{0110} = \frac{5(4\Gamma^2 - 24\Gamma + 99)}{16\beta_1};
\end{aligned}$$

and the third-order coefficients are given by

$$\begin{aligned}
b^{(1)}_{0300} =& -\frac{1}{1536\beta_2}(176\Gamma^4 - 26684\Gamma^3 + 88560\Gamma^2\\
& - 145215\Gamma + 788400),\\
b^{(1)}_{2100} =& \frac{1}{\beta_4}(328\Gamma^5 - 12528\Gamma^4 + 98154\Gamma^3\\
& - 254880\Gamma^2 - 151875\Gamma + 1245375),\\
b^{(1)}_{0120} =& -\frac{1}{\beta_4}(432\Gamma^6 - 2376\Gamma^5 - 28588\Gamma^4 + 431550\Gamma^3\\
& - 2477700\Gamma^2 + 6773625\Gamma - 7948125),\\
b^{(1)}_{0102} =& \frac{1}{16\beta_2}(80\Gamma^5 - 356\Gamma^4 + 11976\Gamma^3 - 81633\Gamma^2\\
& + 111150\Gamma + 83700),\\
b^{(1)}_{1011} =& \frac{1}{\beta_3}(136\Gamma^5 - 1464\Gamma^4 + 8658\Gamma^3 - 21942\Gamma^2\\
& + 36855\Gamma - 46575),\\
b^{(2)}_{0003} =& \frac{5}{16\beta_2}(16\Gamma^5 + 44\Gamma^4 + 2840\Gamma^3 - 12813\Gamma^2\\
& - 10350\Gamma + 2700),\\
b^{(2)}_{2001} =& -\frac{1}{\beta_4}(1304\Gamma^5 - 8736\Gamma^4 + 8190\Gamma^3 + 143100\Gamma^2\\
& - 658125\Gamma + 151875),\\
b^{(2)}_{0201} =& \frac{15(16\Gamma^4 + 1228\Gamma^3 - 7216\Gamma^2 + 18915\Gamma - 18000)}{512\beta_2},\\
b^{(2)}_{0021} =& \frac{1}{\beta_4}(656\Gamma^6 - 20664\Gamma^5 + 185100\Gamma^4 - 757710\Gamma^3\\
& + 1479600\Gamma^2 - 1387125\Gamma + 1366875),\\
b^{(2)}_{1110} =& \frac{1384\Gamma^4 - 8568\Gamma^3 - 342\Gamma^2 + 196830\Gamma - 431325}{32\beta_3}.
\end{aligned}$$

ACKNOWLEDGMENTS

T.S. is partially supported by the Japan Society for the Promotion of Science (JSPS), Grant-in-Aid for Young Scientists (A) #17684002 and Grant-in-Aid for Exploratory Science, # 19654014. K.Y. is partially supported by the JSPS, Grant-in-Aid for Scientific Research (C) #18560056.

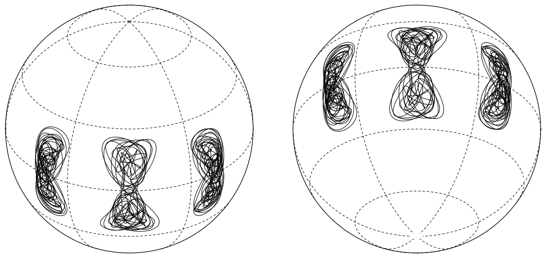

FIG. 4: Chaotic motion of the eight point vortices in the π_e invariant system, which corresponds to the orbit in Fig. 3.

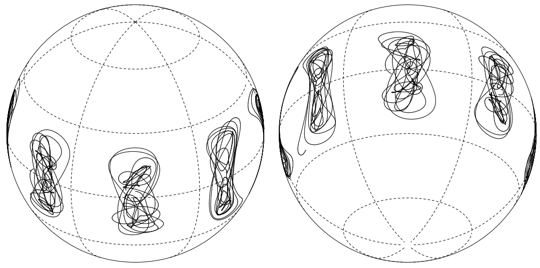

FIG. 5: Chaotic motion of the eight point vortices in the full system (1).

[1] V.I. Arnold, Mathematical Methods of Classical Mechanics, 2nd. ed., Springer, New York, 1989.

[2] S. Boatto and H.E. Cabral, Nonlinear stability of a latitudinal ring of point-vortices on a nonrotating sphere, SIAM J. Appl. Math. 64 (2003) 216–230.

[3] H.E. Cabral, K.R. Meyer and D.S. Schmidt, Stability and bifurcation of the $N+1$ vortex problem on sphere, Regular Chaotic Dyn. 8 (2003) 259–282.

[4] J.R. Dormand and P.J. Prince, Practical Runge-Kutta processes, SIAM J. Sci. Stat. Comput. 10 (1989) 977–989.

[5] E. Doedel, A.R. Champneys, T.F. Fairgrieve, Y.A. Kuznetsov, B. Sandstede and X. Wang, AUTO97: Continuation and Bifurcation Software for Ordinary Differential Equations (with HomCont), 1997, available by anonymous ftp from `ftp.cs.concordia.ca`, directory `pub/doedel/auto`.

[6] S.M. Graff, On the conservation of hyperbolic invariant tori for Hamiltonian systems, J. Diff. Eqns. 15 (1974) 1–69.

[7] J. Guckenheimer and P. Holmes, Nonlinear Oscillations, Dynamical Systems, and Bifurcations of Vector Fields, Springer, New York, 1983.

[8] E. Hairer, S.P. Nørsett, G. Wanner, Solving Ordinary Differential Equations I, 2nd ed., Springer, Berlin, 1993.

[9] A. Jorba, Numerical computation of the normal behaviour of invariant curves of n-dimensional maps, Nonlinearity 14 (2001) 943–976.

[10] R. Kidambi and P.K. Newton, Motion of three point vortices on a sphere, Physica D 116 (1998) 95–134.

[11] C.C. Lim, J. Montaldi, and M. Roberts, Relative equilibria of point vortices on the sphere, Physica D 148 (2001) 97–135.

[12] K.R. Meyer and G.R. Hall, Introduction to Hamiltonian Dynamical Systems and the N-Body Problem, Springer, New York, 1992.

[13] J. Moser, Stable and Random Motions in Dynamical Systems, Princeton Univ. Press, 1973.

[14] P.K. Newton, The N-vortex problem, Analytical techniques, Springer, New York, 2001.

[15] H.E. Nusse and J.A. Yorke, Dynamics: Numerical Explorations, 2nd ed., Springer, New York, 1997.

[16] L.M. Polvani and D.G. Dritschel, Wave and vortex dynamics on the surface of a sphere, J. Fluid Mech. 255 (1993) 35–64.

[17] J. Pöschel, Über invariant Tori in Differenzierbaren Hamiltonschen Systemen, Bonn Math. Schr. 120, Universität Bonn, Bonn, 1980.

[18] T. Sakajo, The motion of three point vortices on a sphere, Japan J. Indust. Appl. Math. 16 (1999) 321–347.

[19] T. Sakajo, Motion of a vortex sheet on a sphere with pole vortices, Phys. Fluids 16 (2004) 717–727.

[20] T. Sakajo, Transition of global dynamics of a polygonal vortex ring on a sphere with pole vortices, Physica D 196 (2004) 243–264.

[21] T. Sakajo, Invariant dynamical systems embedded in the N-vortex problem on a sphere with pole vortices, Physica D 217 (2006) 142–152; Erratum, Physica D 225 (2007) 235–236.

[22] T. Sakajo, Integrable four-vortex motion on sphere with zero moment of vorticity, Phys. Fluids 19 (2007) 017019.

[23] T. Sakajo and K. Yagasaki, Chaotic motion of the N-vortex problem on a sphere: I. Saddle centers in two-degree-of-freedom Hamiltonian, submitted to J. Nonlinear Sci. (2007).

[24] H. Waalkens, A. Burbanks and S. Wiggins, A computational procedure to detect a new type of high-dimensional chaotic saddle and its application to the 3D Hill's problem, J. Phys. A 37 (2004) L257–L265.

[25] S. Wiggins, Normally Hyperbolic Invariant Manifolds in Dynamical Systems, Springer, New York, 1994.

[26] K. Yagasaki, Horseshoe in two-degree-of-freedom Hamiltonian systems with saddle-centers, Arch. Rat. Mech. Anal. 154 (2000) 275–296.

[27] K. Yagasaki, Numerical evidence of fast diffusion in a three-degree-of-freedom Hamiltonian system with a saddle-center, Phys. Lett. A 301 (2002) 45–52.

[28] K. Yagasaki, Homoclinic and heteroclinic orbits to invariant tori in multi-degree-of-freedom Hamiltonian systems with saddle-centers, Nonlinearity 18 (2005) 1331–1350.

[29] K. Yagasaki, Numerical computation of stable and unstable manifolds of normally hyperbolic invariant manifolds, in preparation.